CHEMIJA
2026. Vol. 37. No. 3. P. 244–250

ISSN 0235-7216 eISSN 2424-4538
DOI: https://doi.org/10.6001/chemija.2026.37.3.6

Hydrothermal synthesis and luminescence of Eu^{3+}-doped $Gd_{1-x}La_xPO_4$ phosphates

Monika Rimkienė,

Ramūnas Skaudžius*

Institute of Chemistry,
Department of Inorganic Chemistry,
Faculty of Chemistry and Geosciences,
Vilnius University, 24 Naugarduko Street,
03225 Vilnius, Lithuania

Eu^{3+}-doped gadolinium, lanthanum and mixed gadolinium–lanthanum phosphates were synthesised by a hydrothermal method and investigated as luminescent phosphate materials. The target compositions included $GdPO_4$, $LaPO_4$ and $Gd_{1-x}La_xPO_4$ doped with 15 mol% Eu^{3+}; selected $GdPO_4$:Eu^{3+} samples were also prepared in the presence of sodium lauryl sulfate as a surfactant. X-ray diffraction showed the formation of hydrated phosphate phases. $GdPO_4 \cdot H_2O$:Eu^{3+} samples crystallised in a hexagonal hydrated phase, whereas increasing La content promoted mixtures of hexagonal and monoclinic phases. Photoluminescence measurements confirmed Eu^{3+}-related excitation and emission transitions, with orange–red emission under near–UV excitation. The strongest emission was observed for $GdPO_4 \cdot H_2O$:Eu^{3+}, while increasing surfactant content and increasing La substitution reduced emission intensity. Scanning electron microscopy revealed that agglomerated fine particles and partially elongated particles were formed. Thermal analysis indicated dehydration below approximately 500°C and suggested structural transformation at higher temperatures. The results show that hydrothermal synthesis yields luminescent Eu^{3+}-doped hydrated phosphate materials, but further optimisation is required to obtain phase-pure monoclinic products and controlled morphology.

Keywords: gadolinium phosphate, lanthanum phosphate, europium, hydrothermal synthesis, luminescence, rare-earth phosphates

INTRODUCTION

Multifunctional inorganic materials that combine magnetic and luminescent properties are of interest because they may be applied in optical materials, sensors, scintillators, drug delivery and related technologies [1, 2]. Among such systems, rare-earth orthophosphates are attractive hosts for lanthanide doping because of their thermal and chemical stability, relatively low toxicity and suitable optical properties. In particular, $GdPO_4$ and $LaPO_4$ doped with Eu^{3+} ions are promising matrices for orange–red luminescence [3–6].

Rare-earth phosphate materials may crystallise in hydrated hexagonal structures or in anhydrous monoclinic structures. In $GdPO_4 \cdot H_2O$, the hexagonal structure contains water molecules in channels formed along the crystallographic direction, whereas the monoclinic structure does not contain crystallised water. Similar structural behaviour is observed for lanthanum phosphate. Temperature is one of the key factors controlling the transition from hydrated to anhydrous phosphate phases, because removal of crystallisation water can promote transformation to monoclinic structures [7].

Eu^{3+} ions are efficient luminescent activators in phosphate hosts. Their emission is associated with characteristic $^5D_0 \rightarrow {}^7F_J$ transitions and typically appears in the orange–red spectral region. The luminescence intensity and colour coordinates may depend on host compositiofn, crystal structure, hydration state, surface chemistry and particle morphology [8–12]. Previous phosphate studies have

* Corresponding author. Email: ramunas.skaudzius@chgf.vu.lt

also addressed phosphate-based luminescent systems, and phosphate materials have been considered as compounds that may be incorporated into wood matrices [13–15]. The aim of this work was to synthesise Eu^{3+}-doped $LnPO_4$ (Ln = Gd, La) and $Gd_{1-x}La_xPO_4$ phosphates by a hydrothermal method and to investigate their structure, morphology, thermal behaviour and luminescent properties.

EXPERIMENTAL

Materials

Gd_2O_3 (99.9%, Acrosorganics), La_2O_3 (99.9%, REacton), Eu_2O_3 (99.9%, Acros Organics), $(NH_4)_2HPO_4$ (Eurochemicals), concentrated HNO_3 (Eurochemicals), citric acid monohydrate (99.9%, Chempur), tartaric acid (99.9%, Chempur) and sodium lauryl sulfate were used as starting materials.

Synthesis

$LaPO_4$, $GdPO_4$ and mixed $Gd_{1-x}La_xPO_4$ phosphates doped with Eu^{3+} were synthesised by the hydrothermal route. The corresponding rare-earth oxides and Eu_2O_3 were dissolved in concentrated nitric acid at approximately 70°C under magnetic stirring. When required, a surfactant was added during preparation. After dissolution, excess nitric acid was evaporated and the remaining solution was washed several times with small portions of distilled water. Citric acid was then added, and the pH was adjusted to approximately 2 using diluted NH_4 solution or concentrated HNO_3. A phosphate solution was slowly added, and the mixture was stirred for 30 min. After a final pH adjustment, the solution was transferred to a Teflon-lined autoclave and heated at 180°C for 16 h. The product was sonicated, centrifuged, washed with water and ethanol, and dried for 12 h at 70°C in air.

Characterisation

Powder X-ray diffraction patterns were recorded using a Rigaku Miniflex II diffractometer with Cu radiation and a Ni filter. Measurements were performed in Bragg–Brentano geometry in the 10–80° 2θ range using a 0.02° step and 0.1° s^{-1} scanning rate. Phase identification was carried out using the PDXL software.

Excitation and emission spectra were measured using Edinburgh Instruments FLS900 and FLS920 fluorescence spectrometers equipped with xenon lamps and photomultiplier detectors. Excitation spectra were recorded in the 250–575 nm range while monitoring emission at 586.5 nm. Emission spectra were recorded in the 500–800 nm range using 393 nm excitation.

Scanning electron microscopy was performed using a Hitachi SU–70 field-emission scanning electron microscope at an accelerating voltage up to 10 kV. Samples were prepared by dispersing particles in distilled water and depositing 20 µL of the dispersion on a silicon substrate.

TG-DSC measurements were performed using a PerkinElmer STA 6000 instrument in air at a heating rate of 10°C min^{-1} from 30 to 900°C; the sample mass was approximately 5.5 mg.

RESULTS AND DISCUSSION

Phase composition

X-ray diffraction confirmed that the hydrothermal synthesis produced hydrated rare-earth phosphate phases (Fig. 1). The diffraction peaks of $GdPO_4$:Eu^{3+}

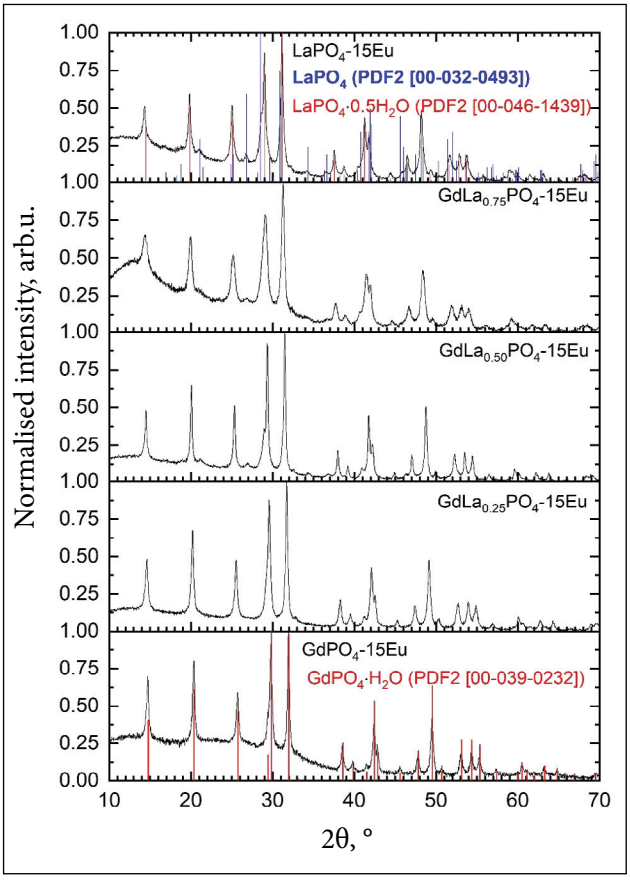

Fig. 1. X-ray diffraction patterns of the synthesised Eu^{3+}-doped $Gd_{1-x}La_xPO_4$:Eu^{3+} powders

corresponded to hexagonal $GdPO_4 \cdot H_2O$ (PDF2 [00–039–0232]). This result is consistent with synthesis in an aqueous medium, where crystallisation water is incorporated into the structure. The $LaPO_4:Eu^{3+}$ sample and the mixed $Gd_{1-x}La_xPO_4:Eu^{3+}$ samples showed composition-dependent phase formation. At 25% La content, a hexagonal phosphate phase was observed. With increasing La content, diffraction patterns indicated mixtures of hexagonal (PDF2 [00-032-0493]) and monoclinic (PDF2 [00-032-0493]) phases, with characteristic monoclinic reflections appearing near 21.1, 26.8 and 28.5° 2θ. The overlap of hexagonal and monoclinic reflections was particularly visible in the 35–70° 2θ range.

The addition of sodium lauryl sulfate during the $GdPO_4:Eu^{3+}$ synthesis did not change the crystal phase (Fig. 2). In all surfactant-containing samples, a hexagonal hydrated phase was obtained, no additional reflections were detected, and the peak width remained nearly unchanged. Therefore, under the applied conditions the surfactant did not significantly affect the phase formation or crystallite size.

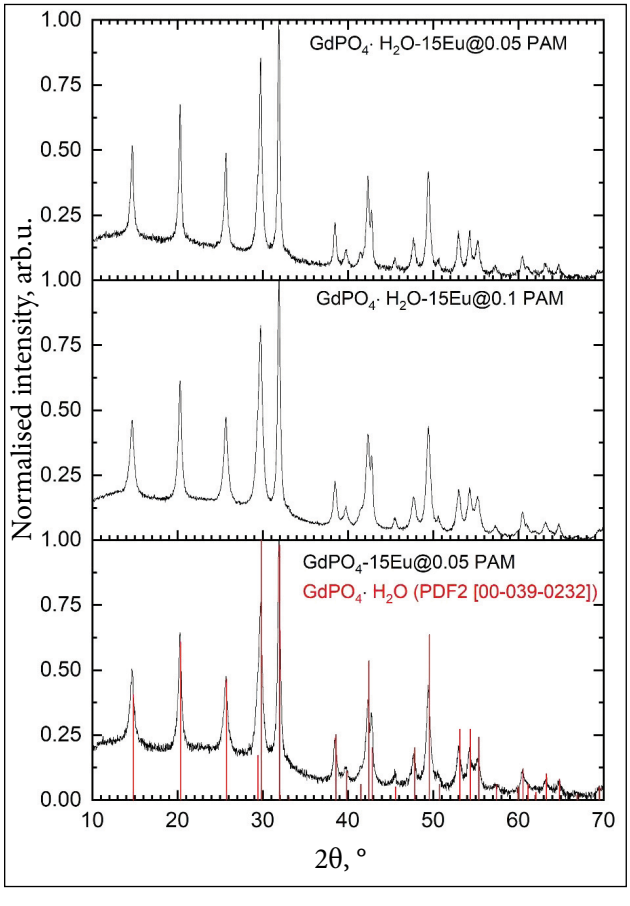

Fig. 2. X-ray diffraction analysis of the synthesised $GdPO_4:Eu^{3+}$ compounds with an additionally added surfactant

Photoluminescence properties

The excitation spectra recorded at 587 nm emission contained bands attributed to Gd^{3+} and Eu^{3+} ions (Fig. 3). The charge-transfer band associated with $O^{2-} \rightarrow Eu^{3+}$ transitions was observed in the ultraviolet region, while the most intense Eu^{3+} excitation band appeared near 395 nm and was assigned to the $^7F_0 \rightarrow {}^5L_5$ transition. Additional Eu^{3+}–related excitation bands were observed near 460 and 525 nm, corresponding to $^5F_4 \rightarrow {}^7L_6$ and $^5F_4 \rightarrow {}^7L_4$ transitions, respectively.

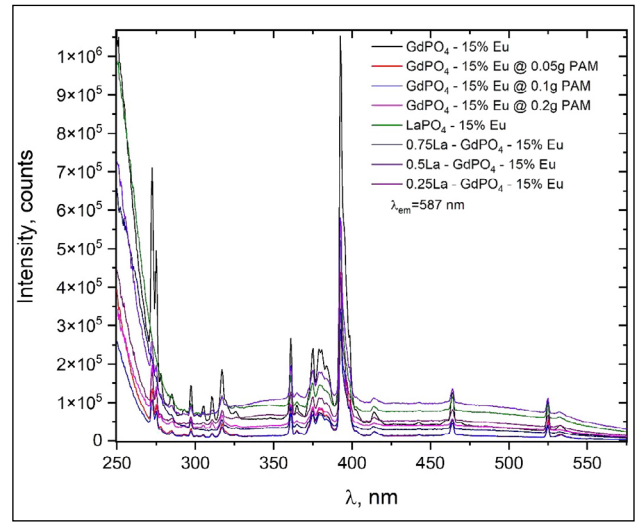

Fig. 3. Excitation spectra of $Gd_{1-x}La_xPO_4:Eu^{3+}$ samples with different compositions

Emission spectra recorded under 393 nm excitation showed characteristic Eu^{3+} transitions (Fig. 4). Less intense bands near 585, 610 and 650 nm were assigned to the $^5D_0 \rightarrow {}^7F_1$, $^5D_0 \rightarrow {}^7F_2$ and $^5D_0 \rightarrow {}^7F_3$ transitions, respectively. The most intense emission occurred near 700 nm and was attributed to the $^5D_0 \rightarrow {}^7F_4$ transition. The positions of Eu^{3+} emission bands did not change significantly with La substitution, indicating that the local Eu^{3+} emission environment remained broadly similar.

The highest luminescence intensity was observed for $GdPO_4:Eu^{3+}$. Increasing La content decreased the emission intensity, although the spectral shape remained similar. The use of surfactant also reduced both excitation and emission intensity; a higher surfactant content led to a weaker luminescence. This effect is consistent with the presence of organic molecules that may absorb incoming and emitted radiation [16].

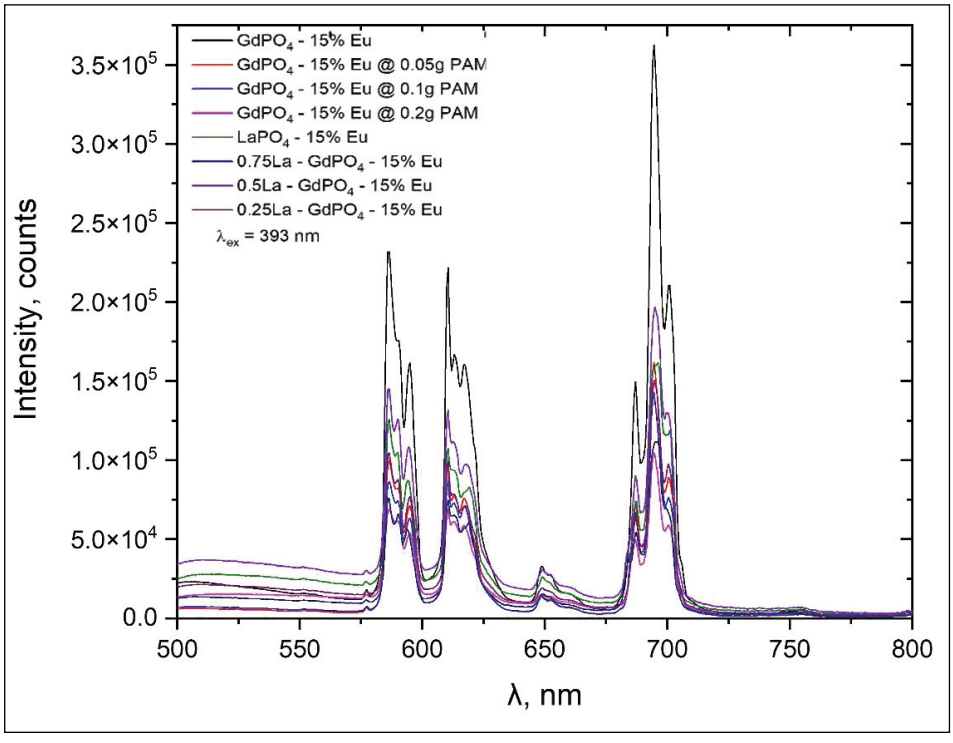

Fig. 4. Emission spectra of $Gd_{1-x}La_xPO_4:Eu^{3+}$ samples with different compositions

CIE colour coordinates

CIE colour coordinates calculated from emission spectra confirmed that the synthesised samples emitted in the orange–red region. The coordinates were located approximately between (0.48, 0.49) and (0.41, 0.58), corresponding to emission wavelengths in the range of approximately 577–591 nm. Points 1–3 correspond to $GdPO_4$–15Eu@xPAM, point 4 to $GdPO_4$–15Eu, point 5 to $LaPO_4$–15Eu, and points 6–8 to $Gd_{1-x}La_xPO_4$ with La contents of 0.75, 0.50 and 0.25, respectively. La incorporation caused a small shift towards the orange region, but all samples remained within the orange–red emission range.

Morphology

SEM analysis showed that the expected nanowire morphology was not formed under the applied synthesis conditions. Most samples consisted of very fine, agglomerated particles without clear boundaries. Agglomerates varied in size, and

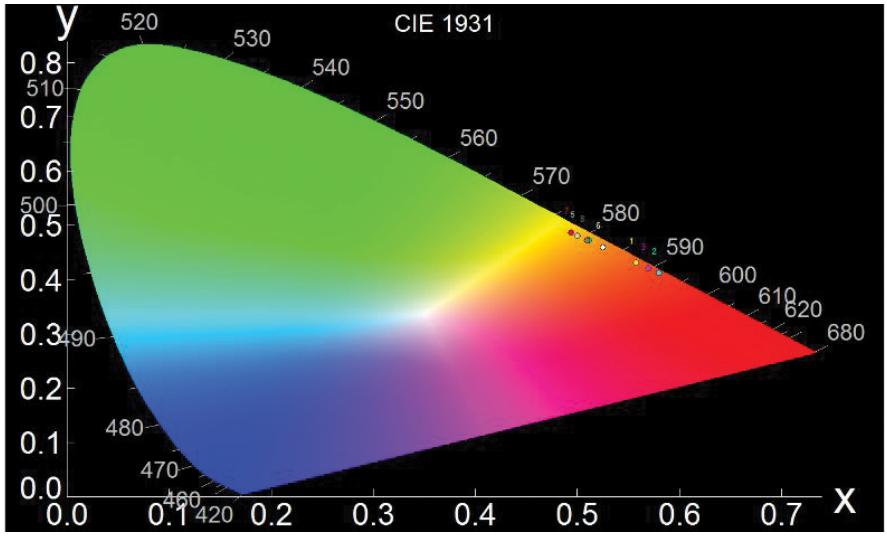

Fig. 5. CIE colour coordinates of the synthesised phosphates

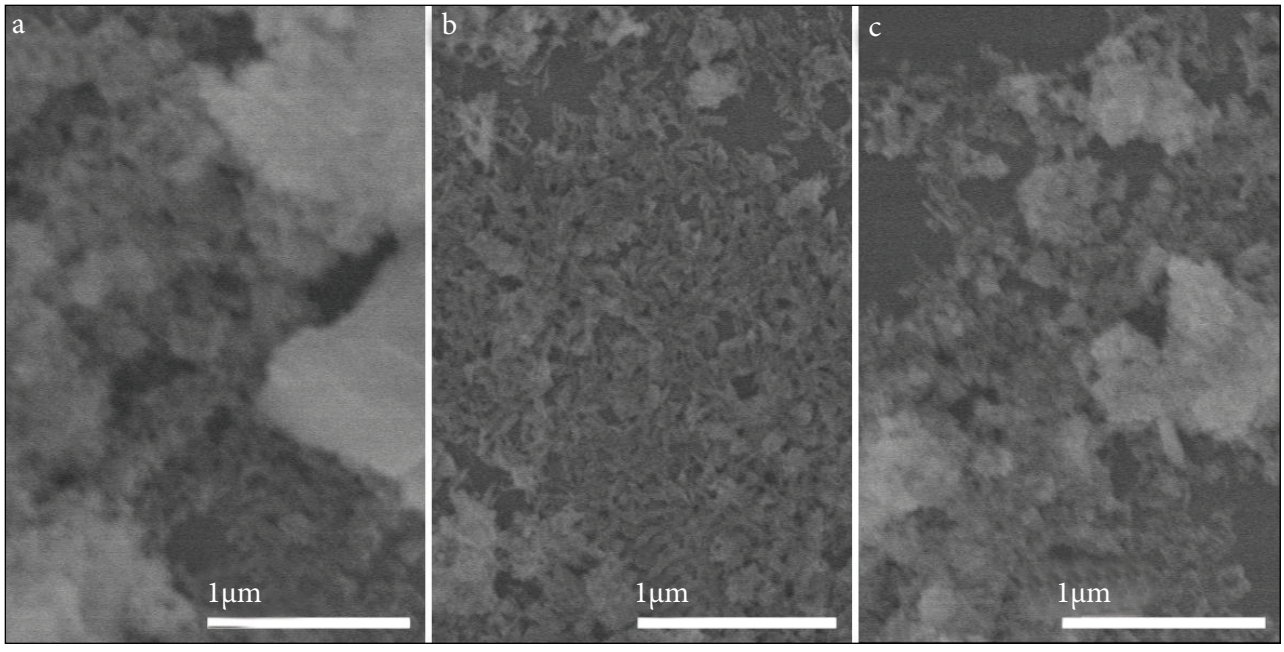

Fig. 6. SEM images of $GdPO_4 \cdot H_2O$. Samples were prepared by adding different amounts of surfactant: (a) 0.05 g surfactant, (b 0.1 g surfactant, (c) 0.2 g surfactant

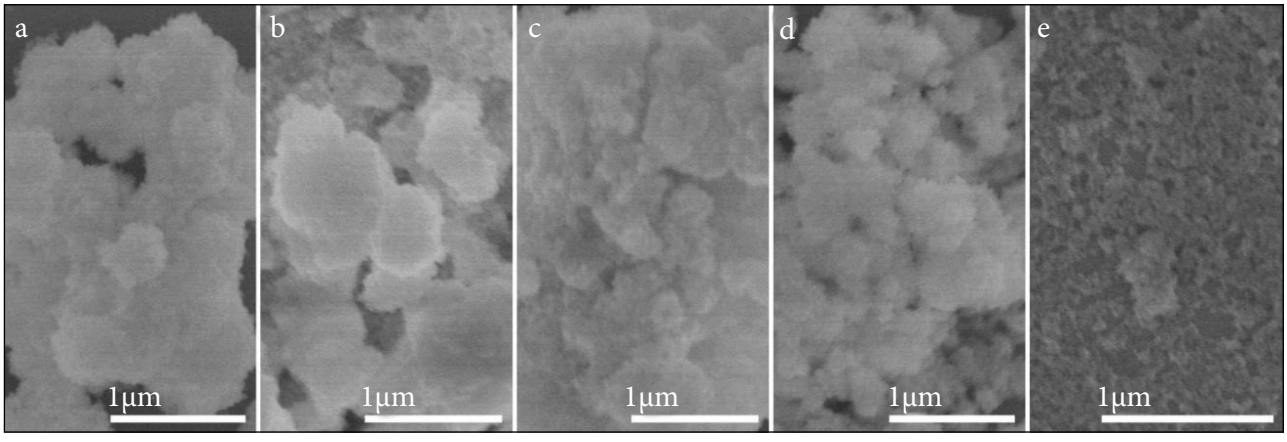

Fig. 7. SEM images of $Gd_{1-x}La_xPO_4:Eu^{3+}$. Samples were prepared with different amounts of lanthanum: (a) $GdPO_4:Eu^{3+}$, (b) $Gd_{0.75}La_{0.25}PO_4:Eu^{3+}$, (c) $Gd_{0.5}La_{0.5}PO_4:Eu^{3+}$, (d) $Gd_{0.25}La_{0.75}PO_4:Eu^{3+}$, (e) $LaPO_4:Eu^{3+}$

some reached the micrometre scale, whereas other particles were around 0.5 μm. Only traces of nanowire-like growth were observed in the sample prepared with 0.1 g of a surfactant.

In the samples with higher La content and in $LaPO_4:Eu^{3+}$, the particles became finer and somewhat more elongated, but well-defined nanowires were still not obtained.

Thermal behaviour

TG-DSC analysis was used to evaluate the dehydration of hydrated phosphate phases (Fig. 8). For $GdPO_4 \cdot H_2O$, the expected water content is 6.67%; experimentally, the total mass loss was about 5.5%. The first mass decrease occurred between 30 and 145°C and amounted to approximately 1.5%. A sharper mass loss of about 2.5% was observed between 145 and 200°C, accompanied by an endothermic peak near 190°C. The mass stabilised at approximately 500°C, indicating that this temperature range is required to remove crystallisation water. Above 600°C, an exothermic process was observed and was attributed to possible transformation from the hexagonal hydrated structure to a monoclinic phase. A similar dehydration process was observed for $LaPO_4 \cdot 0.5H_2O$ where the total mass loss was approximately 6% (Fig. 9).

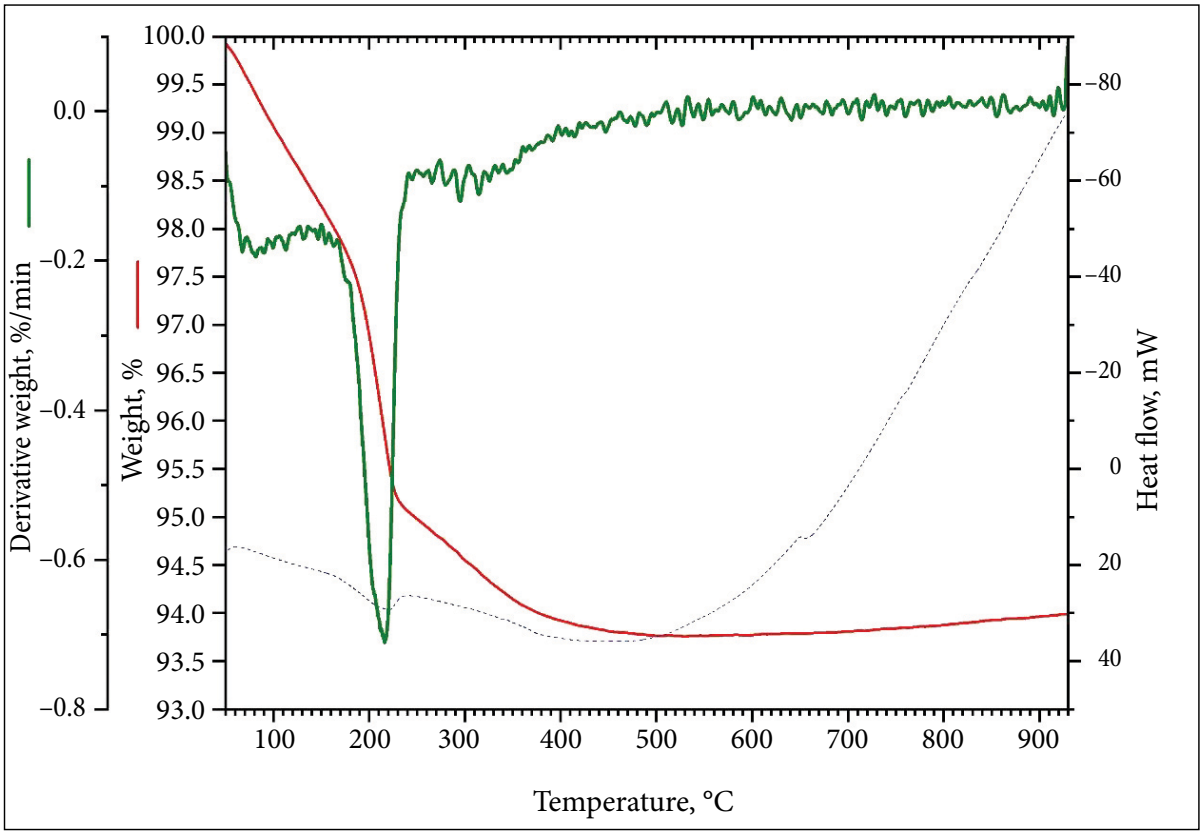

Fig. 8. TG-DTG-DSC curves of $GdPO_4 \cdot H_2O$: red TG, green DTG, blue DSC

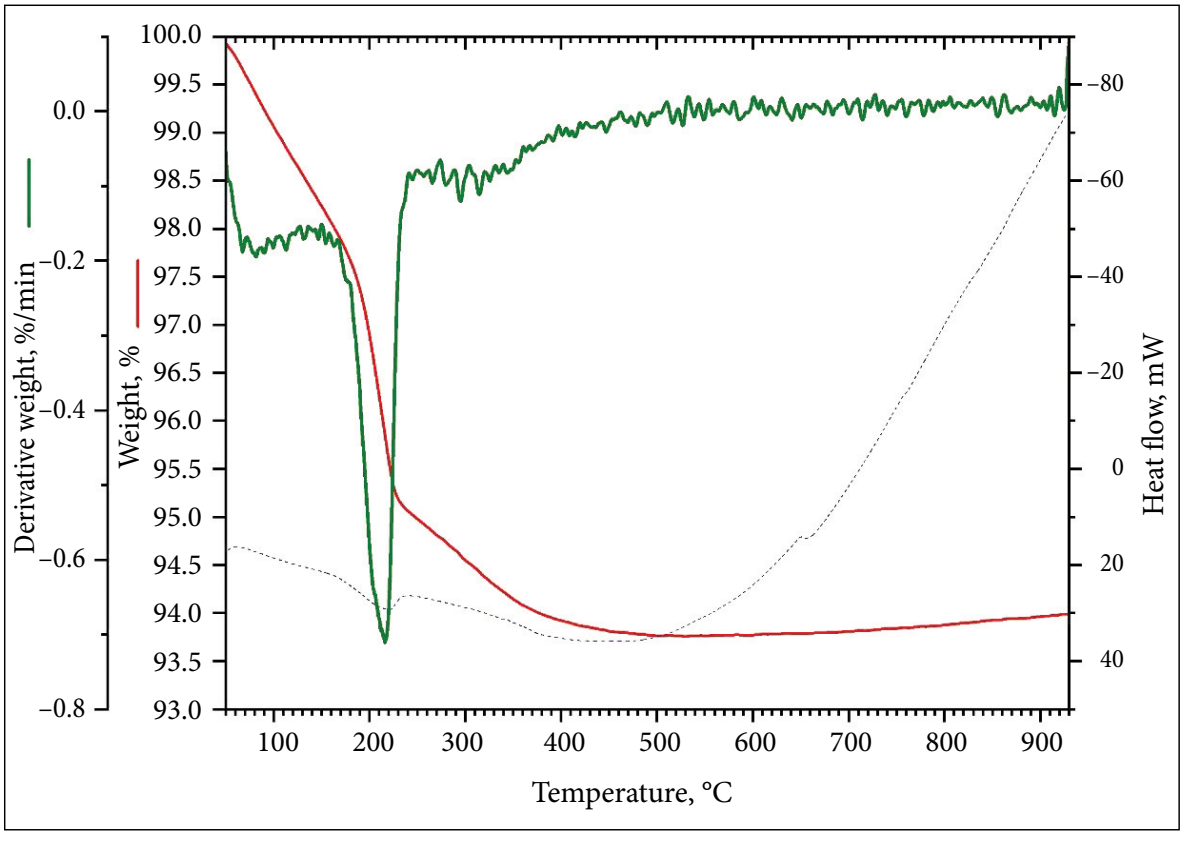

Fig. 9. TG-DTG-DSC curves of $LaPO_4 \cdot 0.5H_2O$: red TG, green DTG, blue DSC

CONCLUSIONS

Eu^{3+}-doped $GdPO_4 \cdot H_2O$, $LaPO_4 \cdot 0.5H_2O$ and mixed $Gd_{1-x}La_xPO_4 \cdot H_2O$ phosphates were successfully synthesised by a hydrothermal method. X-ray diffraction confirmed the formation of hydrated rare-earth phosphate phases under the applied synthesis conditions. $GdPO_4$:Eu^{3+} crystallised in a hexagonal hydrated structure, whereas increasing La content promoted the coexistence of hexagonal and monoclinic phases. The addition of sodium lauryl sulfate did not significantly affect the crystal phase of $GdPO_4$:Eu^{3+}.

Photoluminescence measurements showed characteristic Eu^{3+} excitation and emission transitions, and all synthesised samples exhibited orange–red emission. The highest emission intensity was observed for $GdPO_4$:Eu^{3+}, while both La substitution and increasing surfactant content reduced the luminescence intensity. The SEM analysis showed that the targeted nanowire morphology was not achieved; the products mainly consisted of agglomerated fine particles, with only partial elongation in selected samples. TG-DSC analysis indicated dehydration below approximately 500°C and suggested a possible structural transformation above 600°C. These results show that the hydrothermal route is suitable for obtaining luminescent Eu^{3+}-doped hydrated phosphate materials, although further optimisation is required to obtain phase-pure monoclinic products with controlled morphology.

Received 16 July 2026
Accepted 22 July 2026

References

1. A. G. Hernández, D. Boyer, A. Potdevin, et al., *Phys. Status Solidi A*, **211**, 498 (2014).
2. H. Guo, F. Li, R. Wei, H. Zhang, C. Ma, *J. Am. Ceram. Soc.*, **95**, 1178 (2012).
3. B. Yan, X. Xiao, *Nanoscale Res. Lett.*, **5**, 1962 (2010).
4. L. Yu, D. Li, M. Yue, J. Yao, S. Lu, *Chem. Phys.*, **326**, 478 (2006).
5. L. Yu, H. Song, S. Lu, Z. Liu, L. Yang, X. Kong, *J. Phys. Chem. B*, **108**, 16697 (2004).
6. V. Kumar, S. Singh, R. K. Kotnala, S. Chawla, *J. Lumin.*, **146**, 486 (2014).
7. S. K. Gupta, P. S. Ghosh, M. Sahu, K. Bhattacharyya, R. Tewari, V. Natarajan, *RSC Adv.*, **5**, 58832 (2015).
8. M. Janulevičius, V. Klimkevičius, A. Vanetsev, V. Plausinaitienė, S. Sakirzanovas, A. Katelnikovas, *Mater. Today Commun.*, **23**, 100934 (2020).
9. M. Norkus, M. Skruodienė, G. Niaura, A. Šarakovskis, R. Skaudžius, *J. Non-Cryst. Solids*, **569**, 120966 (2021).
10. D. Budrevičius, R. Skaudžius, *J. Alloys Compd.*, **911**, 164963 (2022).
11. D. Budrevičius, N. Kajimoto, A. Pakalniškis, K. Tsuru, A. Kareiva, R. Skaudžius, *Ceram. Int.*, **49**, 2373 (2023).
12. D. Budrevičius, E. Buzaitytė, K. Mažeika, R. Skaudžius, *Crystals*, **15**, 441 (2025).
13. M. Baublytė, A. Vailionis, D. Sokol, R. Skaudžius, *Ceram. Int.*, **49**, 31255 (2023).
14. M. Baublytė, D. Sokol, K. Mažeika, et al., *Ceram. Int.*, **51**, 27814 (2025).
15. M. Baublytė, E. Paradisi, C. Leonelli, et al., *Inorg. Chem. Commun.*, **183**, 115887 (2026).
16. Z. Huo, C. Chen, D. Chu, H. Li, Y. Li, *Chem. Eur. J.*, **13**, 7708 (2007).

Monika Rimkienė, Ramūnas Skaudžius

Eu^{3+} JONAIS LEGIRUOTŲ $Gd_{1-x}La_xPO_4$ FOSFATŲ HIDROTERMINĖ SINTEZĖ IR LIUMINESCENCINĖS SAVYBĖS

S a n t r a u k a

Darbe hidroterminiu metodu susintetinti Eu^{3+} jonais legiruoti gadolinio, lantano ir mišrūs gadolinio–lantano fosfatai. Rentgeno spindulių difrakcinė analizė parodė, kad susidarė hidratuotos fosfatų fazės: $GdPO_4$:Eu^{3+} mėginyje vyravo heksagoninė hidratuota fazė, o didėjant lantano kiekiui formavosi heksagoninės ir monoklininės fazių mišiniai. Liuminescencijos tyrimai patvirtino Eu^{3+} jonams būdingus sužadinimo ir emisijos perėjimus, o mėginiai skleidė oranžinę–raudoną šviesą. Didžiausias emisijos intensyvumas nustatytas $GdPO_4$:Eu^{3+} mėginyje, o didėjantis lantano ir paviršių aktyviosios medžiagos kiekis emisiją silpnino. SEM tyrimai parodė, kad tikėta nanovielų morfologija nesusiformavo – gautos smulkios aglomeruotos dalelės. TG–DSC analizė parodė, kad kristalizacinis vanduo pasišalina iki maždaug 500 °C, o aukštesnėje temperatūroje galimas struktūros virsmas.